# CNS-specific Expression of C3a and C5a Exacerbate Demyelination Severity in the Cuprizone Model[1]

**Sarah A. Ingersoll**[a,b], **Carol B. Martin**[c], **Scott R. Barnum**[d], and **Brian K. Martin**[b,c,e]

Sarah A. Ingersoll: sarah-ingersoll@uiowa.edu; Scott R. Barnum: sbarnum@uab.edu; Brian K. Martin: cmartin@linkp.com

[a] Interdisciplinary Graduate Program in Immunology, University of Iowa, 357 Medical Research Center, Iowa City, IA 52242

[b] Iowa Cancer Research Foundation, 11043 Aurora Ave, Urbandale, IA, 50322

[c] NewLink Genetics, 2901 South Loop Dr., Ames, IA 50010

[d] Department of Microbiology, University of Alabama at Birmingham, Birmingham, AL 35294

## 1. Introduction

Activation of any of the complement pathways results in the downstream production of two small protein cleavage products, C3a and C5a, collectively known as anaphylatoxins. C3a and C5a are known to induce proinflammatory functions such as chemotaxis, upregulation of cytokine and chemokine production, and enhanced phagocytosis (Haas and van Strijp, 2007). C3a and C5a mediate their effects by binding to their receptors, C3aR and C5aR (CD88), which are expressed on a wide variety of cell types, including glial cells of the CNS. Anaphylatoxins also bind C5a receptor-like 2 (C5L2), whose functions have not been clearly defined, but may act as a decoy or scavenger receptor (Klos et al., 2009). Previous studies have shown that astrocytes, microglia, neurons and oligodendrocytes express anaphylatoxin receptors (Davoust et al., 1999; Gasque et al., 1997; Gavrilyuk et al., 2005; Nataf et al., 2001). C3a and C5a signaling in the CNS can induce a wide range of functions depending upon the cell type and local environmental stimuli. The overall effect of C3a and/ or C5a signaling on glial cell subsets and during CNS disease pathology can be complex, because these proteins have proven to be both protective and harmful. For instance, C5a has been shown to protect neurons against glutamate-mediated apoptosis both *in vitro* and *in vivo* (Mukherjee et al., 2008; Osaka et al., 1999b). Additionally, C3a has been implicated in neural stem cell regeneration and migration (Rahpeymai et al., 2006; Shinjyo et al., 2009). In contrast, C3a and C5a have been shown to have exacerbating effects on CNS disease severity in mouse models of Alzheimer's (Fonseca et al., 2009), amyotrophic lateral sclerosis (ALS) (Woodruff et al., 2008) and lupus (Jacob et al., 2010a; Jacob et al., 2010b). Several studies have also suggested that complement may play a role in the neurodegenerative disease, multiple sclerosis (MS) (Ingram et al., 2008).

[1] Abbreviations used in this paper: EAE, experimental allergic encephalomyelitis; LFB-PAS, Luxol Fast Blue-Periodic acid Schiff; MS, multiple sclerosis; WT, C57BL/6 wild-type mice; IF, immunofluorescence; GFAP, glial fibrillary acidic protein; RCA, *Rincinus Communis* Agglutinin I; Olig-2, oligodendrocyte transcription factor 2; C3a txg, C3a transgenic; C5a txg, C5a transgenic.

[e] Address correspondence and reprint requests to: Brian K. Martin, Ph.D., Iowa Cancer Research Foundation, 11043 Aurora Ave., Urbandale, IA 50322, bmartin@iowacancer.org, phone: (515) 270-8931, FAX: (515) 270-8934.

MS is a chronic, inflammatory disease that targets the myelin sheath surrounding nerves, affecting nerve conduction (Trapp and Nave, 2008). There have been several studies showing that complement proteins, including C3a, contribute to the pathogenesis of demyelination. Glial cells are able to produce complement proteins, so it is possible for localized activation of complement pathways to occur in the CNS (Sospedra and Martin, 2005). C3aR and C5aR are expressed in areas of inflammation in the CNS of MS patients (Gasque et al., 1997; Gasque et al., 1998; Muller-Ladner et al., 1996). In EAE, a mouse model of multiple sclerosis, C3a and C3aR have been shown to play a role in exacerbating disease severity (Boos et al., 2004). Interestingly, it has been shown that C5a and C5aR do not play a role in EAE pathology (Reiman et al., 2005; Reiman et al., 2002). Results from our lab have determined that complement plays a role in the murine cuprizone-mediated demyelination and remyelination model. When a soluble CNS-specific form of the rodent complement regulatory protein, Crry (sCrry) was expressed, mice were protected from demyelination during cuprizone treatment, implicating a role for C3 and downstream complement proteins in this model (Briggs et al., 2007). In our current studies, we utilized the murine cuprizone model to assess the role of local C3a and C5a production in the brain during demyelination and remyelination.

Cuprizone is a copper chelating drug that when given at low doses in the diet of C57BL/6 mice, leads to apoptosis of oligodendrocytes, the myelin producing cells of the brain (Mason et al., 2000). The death of these cells results in demyelination in predictable, specific axonal tracts of the brain, including the corpus callosum, cerebellum and the superior cerebellar peduncle (Groebe et al., 2009; Matsushima and Morell, 2001). One attractive aspect of the cuprizone model is the relative lack of blood brain barrier breakdown (Bakker and Ludwin, 1987; Kondo et al., 1987), which makes it possible to analyze the local response of glia to C3a or C5a production. The primary effector cells in demyelination during treatment with cuprizone are reactive astrocytes and microglia. Demyelination in this model shares some characteristics with type III and IV lesions described in MS (Lucchinetti et al., 2000), characterized by oligodendrocyte death, microglial infiltration and lack of antibodies present in areas of demyelination. After mice are returned to a normal diet, the affected areas in the brain undergo remyelination, allowing for the investigation of events that occur during remyelination pathogenesis. We utilized transgenic mice expressing C3a or C5a under the control of the CNS-specific GFAP promoter to determine the role of C3a and C5a production on demyelination and remyelination events.

C3a and C5a are able to act as chemotactic factors; therefore, we hypothesized that an increase in the expression of C3a and C5a in transgenic mice being treated with cuprizone would exacerbate demyelination severity by increasing the number of inflammatory cells migrating into the corpus callosum. In contrast to results observed in the EAE model, we found that both C3a and C5a played a role in increased demyelination pathology. Both C3a and C5a transgenic mice had increased microglia in the corpus callosum during demyelination. Interestingly, when cuprizone was removed from the diet, oligodendrocytes returned to the demyelinated corpus callosum in higher numbers in C3a and C5a transgenic mice, thus allowing for complete remyelination of the corpus callosum. When we investigated the effect of C3a and/or C5a on individual subsets of glial cells, we found an increase in proinflammatory cytokine and chemokine production, indicating an ability of C3a and C5a to induce proinflammatory effects in glial cells.

## 2. Materials and Methods

### 2.1. Mice

Previously described C3a-GFAP (Boos et al., 2004) and C5a-GFAP (Reiman et al., 2005) transgenic mice on the C57BL/6 background were provided by S. R. Barnum (University of

Alabama). Five week old male C57BL/6 mice were purchased from Jackson Laboratories, Bar Harbor, ME.

## 2.2. Induction of Demyelination and Remyelination

To induce demyelination, 8–12 week old male mice were fed a diet of NIH-31 Modified 6% Mouse/Rat Sterilizable Diet-meal form (Harlan Laboratories, Madison, WI), containing 0.2% cuprizone (bis (cyclohexanone) oxaldihydrazone, Sigma-Aldrich, St. Louis, MO) for six weeks. Mice were returned to a normal diet after six weeks of cuprizone treatment to allow for remyelination (Briggs et al., 2007; Matsushima and Morell, 2001; Morell et al., 1998).

## 2.3 Histological Analysis

Tissue processing and microscopy were carried out as previously described (Arnett et al., 2001; Briggs et al., 2007). Briefly, mice were anesthetized and transcardially perfused with PBS, followed by 4% paraformaldehyde. Brains were then removed and incubated in 4% paraformaldehyde for seven days and embedded in paraffin. Five micrometer coronal sections corresponding to Sidman sections 241–251 (Sidman, 1971) were used for histological analyses. All demyelination and remyelination studies using Luxol Fast Blue-Periodic acid Schiff (LFB-PAS) were done at midline of the corpus callosum. A demyelination severity score of zero indicates no demyelination, while a score of three indicates complete demyelination. Each section was scored blindly by three different individuals and the scores averaged for each mouse. Because of the large number of mice used in these studies, sections were stained in two separate groups. Untreated controls were stained along with each group to ensure that staining was consistent between experiments. WT, C3a-GFAP and C5a-GFAP mice from the same timepoint were stained together to guarantee an accurate comparison between WT and the transgenic mice.

## 2.4. Immunohistochemistry

For immunohistochemistry, paraffin sections were rehydrated, heat-unmasked, and then blocked with a solution containing 5% normal goat serum and 0.1% Triton X-100 (Sigma-Aldrich) in PBS. Slides were incubated overnight with primary antibody diluted in blocking solution. Appropriate fluorochrome-labeled secondary antibodies (Invitrogen-Molecular Probes, Carlsbad, CA) were used for detection. The immunohistochemistry antibodies used were: Biotinylated RCA-1 (Vector Laboratories, Burlingame, CA; 1:100), a lectin used to detect microglia/macrophages; the secondary reagent used was streptavidin-Alexa Fluor-594; GFAP was detected using anti-GFAP antibody (Dako, Carpinteria, CA; 1:100); the secondary antibody was goat anti-rabbit Alexa Fluor-488; antibody to the Olig-2 transcription factor (Ligon et al., 2004), a gift from C. D. Stiles (Harvard University), was used at 1:10,000 to detect total oligodendrocytes; the secondary reagent was goat anti-rabbit Alexa Fluor-488. Because of the large number of mice used in these studies, the sections were stained in two separate groups. Untreated controls were stained along with each group to ensure that staining was consistent between experiments. WT, C3a-GFAP and C5a-GFAP mice from the same timepoint were stained together to guarantee an accurate comparison between WT and the transgenic mice. For studies comparing different treatments, all sections were digitally captured by microscopy using the same settings for each experiment. All of the brains were analyzed at midline of the corpus callosum. RCA and GFAP images were analyzed using ImageJ. Olig-2 and DAPI cells were quantified using NIS Elements 3.1 Imaging software (Nikon, Melville, NY). Manipulations of the digital images after capture were performed equally on all pictures.

### 2.5. Glial Cell Lines and Enrichment of Glial cultures

The BV-2 murine macrophage cell line was a gift from Jenny P.-Y. Ting (The University of North Carolina at Chapel Hill). BV-2 cells were cultured in DMEM (Invitrogen) with penicillin–streptomycin (Invitrogen) and 10% fetal bovine serum (Hyclone, Logan, UT). Primary astrocytes were obtained from one to three day-old neonatal mouse brains based on methods previously described (McCarthy and de Vellis, 1980; Nikcevich et al., 1999). Briefly, the brains of one to three day-old mice were dissected, meninges removed and cells dissociated in trypsin–EDTA. Mixed glial cells were cultured for 10–12 days at which time the microglia and oligodendrocytes precursors were shaken off at 225 rpm overnight. Following trypsin–EDTA treatment, astrocytes were cultured on new plates. Enriched astrocytes were >95% GFAP positive by FACS analysis (data not shown). Astrocytes were cultured in DMEM (Invitrogen) with penicillin–streptomycin (Invitrogen) and 10% fetal bovine serum (Hyclone). All animals were housed in the Laboratory of Animal Resources facilities at Iowa State University and all mouse protocols were approved by the Iowa State University Animal Care and Use Committee.

### 2.6. Adenoviral Infection and Purification of C3a- and C5a-FLAG protein

Sequences for murine C3a and C5a were cloned from mouse liver cDNA using reverse-transcription-PCR. A FLAG-tag sequence was cloned at the 5′ end of both minigene constructs for purification and identification purposes. The Genbank accession numbers assigned to C3a and C5a sequences are HM105585 and HM105584, respectively. Since both C3a and C5a are internal sequences within the C3 and C5 genes, respectively, a heterologous signal sequence from the murine IFN-γ gene was included at the 5′ end. The adenoviral vector (pacAd5) was provided by the University of Iowa Gene Transfer Vector Core (GTVC). Each construct included an internal GFP cassette so that transduction efficiency could be monitored. The GTVC performed the adenoviral preparation. The recombinant Ad vector is based on the human adenovirus serotype 5, from which the E1a and E1b replication genes have been deleted in order to make virus replication defective (Anderson et al., 2000). A549 human lung cells were transduced with the adenovirus at high MOI in serum-free Hybridoma SFM media (Invitrogen). After 48 hours, supernatants from transduced cells were collected, filtered and purified over an anti-FLAG-M2-agarose affinity column (Sigma-Aldrich). Proteins were eluted with low pH buffer and eluted proteins along with defined amounts of human C5a were run on a 15% SDS-PAGE gel and visualized by silver stain to quantify the amount of murine C3a or C5a. These proteins were shown to be functional by cell binding experiments and chemotaxis assays (data not shown).

### 2.7. Signaling Assays

Primary astrocytes and BV-2 microglia were treated with 50nM C3a or C5a for 0–60 minutes. At the indicated time, cells were lysed with RIPA buffer (50mM Tris-HCl, pH 7.5, 150mM NaCl, 1mM EDTA, 1% NP-40 and 1% sodium deoxycholate) containing protease inhibitor (Roche Diagnostics, Indianapolis, IN) and phosphatase inhibitor cocktails (Sigma-Aldrich). Protein lysate concentrations were quantified using Bio-Rad Protein Assay reagent (BioRad, Hercules, CA) and equal amounts of protein lysate were loaded and run on a 10% SDS-PAGE gel for 1.5–2 hours. Gels were then transferred onto 45μm PVDF membrane using a semi-dry transfer system. Blots were blocked in 5% fat-free dry milk (w/v) and then incubated overnight in primary antibody (pERK1/2, pJNK or p-p38 MAPK) (Cell Signaling Technology, Danvers, MA). Blots were developed on film using LumiGLO chemiluminesence reagent (Cell Signaling Technology). Blots were then stripped using Restore Western blot stripping buffer (Thermo Fisher Scientific Inc., Rockford, IL), re-blocked and incubated with total ERK1/2, JNK or p38 MAPK antibodies (Cell Signaling Technology). Films were scanned and the densities of the bands were measured using

ImageJ analysis software. Phosphorylated band values were normalized to their respective total band value to account for protein loading differences.

### 2.8. BioPlex and enzyme-linked immunosorbent assay (ELISA)

BV-2 microglia, primary astrocytes and mixed glial cells were plated in six-well tissue culture treated dishes. Primary mixed glial cultures were allowed to mature for 10–12 days before treatment. Cells were treated with 50nM C3a, 50nM C5a or a combination of 50nM of both C3a and C5a for the indicated times. Supernatants were collected from each treatment group and were run in duplicate using a 23-multiplex assay (BioRad). Supernatant IL-6 levels were verified using an ELISA kit (BioLegend, San Diego, CA). CCL4 levels in the supernatants were verified by ELISA (R&D Systems Inc., Minneapolis, MN). Untreated cell supernatants were used as controls for each time point.

### 2.9. Statistics

Student's unpaired t-test (two-tailed distribution, homoscedastic, Microsoft Excel) was used to examine the probability that differences between treatment groups were statistically significant. For the in vivo animal studies, one-way ANOVA was also used to verify the significance in longitudinal studies between different treatment groups.

## 3. Results

### 3.1. Increased levels of C3a and C5a in the brain lead to exacerbated demyelination and delayed remyelination

To determine the role of C3a and C5a in demyelination and remyelination, we used transgenic mice expressing C3a or C5a under the control of the CNS-specific GFAP promoter. Our results show that after four weeks on the cuprizone diet, both C3a and C5a transgenic mice had worse demyelination severity compared to C57BL/6 wild type (WT) mice (Fig. 1A and 1B). Demyelination severity was increased through seven weeks in both transgenic groups (Fig. 1A). Although these mice showed worse demyelination severity at seven weeks, we found that both transgenic groups were able to remyelinate completely by the end of the ten week study (Fig. 1A), suggesting increased C3a or C5a production does not affect the overall ability of these mice to undergo effective remyelination.

Along with increased demyelination severity in the corpus callosum of transgenic mice, we also observed increased cellular infiltration and thickness of the inflammatory lesion within and surrounding the corpus callosum. The increased thickness of the lesion is most likely a result of increased cell migration or cellular proliferation within the demyelinating corpus callosum. When we measured the thickness of the lesion below the midline of the brain, we found that the corpus callosum and surrounding inflammation had almost doubled in width compared to the WT mice at five weeks (Fig. 1B and 1C). We saw no differences in the thickness of the corpus callosum in untreated transgenic mice compared to untreated WT mice (Fig. 1C). Previous results from our lab (unpublished) and others have shown that mice lose weight during cuprizone treatment and regain weight after cuprizone treatment is discontinued (Hiremath et al., 1998; Torkildsen et al., 2008). Throughout the ten week study we found that all groups of mice lost 10–20% of their original weight while on the cuprizone diet. We observed that when mice were put back onto a normal diet after six weeks, the C3a transgenic mice did not regain as much weight as the WT and C5a transgenic mice (Fig. 1D). Interestingly, untreated C3a transgenic mice started the study weighing significantly more than untreated WT and C5a transgenic mice (data not shown). These results may suggest that a currently unknown systemic effect is occurring in the C3a transgenic mice. The C3a degradation product, C3a desArg, also known as acylation-stimulating protein, is involved in lipid biology and can influence body weight (Cianflone et al., 2003). Potentially,

this protein could be playing a role in the weight of C3a transgenic mice throughout development; however it is unknown if C3adesArg is able to escape the blood brain barrier in these mice. Further investigation of this phenomenon will be required to determine the mechanism for overall increased weight over WT mice and decreased weight gain after cuprizone removal in the C3a transgenic mice.

## 3.2 C3a and C5a expression leads to increased cell infiltration into the corpus callosum during cuprizone treatment

It was evident from the LFB-stained sections that there were greater numbers of cells in the demyelinated corpus callosum of the C3a and C5a transgenics compared to WT mice. Using DAPI nuclear stain to quantify the number of cells in the corpus callosum, we found that after five weeks of cuprizone treatment, both transgenic strains had increased numbers of cells compared to WT mice (Fig. 2A and 2B). The cell numbers in the corpus callosum remained elevated in C3a and C5a mice through eight weeks (Fig. 2A). We found no significant changes in the number of cells in the corpus callosum of untreated WT mice compared to untreated C3a and C5a transgenic mice (Fig. 2A and 2B), suggesting there was no preexisting inflammation in the corpus callosum of transgenic mice prior to the cuprizone treatment.

Astrogliosis and microglial infiltration in the corpus callosum during demyelination are well characterized events that occur at predictable time points during cuprizone treatment (Matsushima and Morell, 2001). When GFAP antibody was used to detect astrocytes in the corpus callosum, we found that the GFAP levels in the transgenic mice followed a similar trend compared to the WT mice throughout the ten week study. The increase in GFAP expression in all groups of mice started at three weeks and persisted through eight weeks (Fig. 3A), which implied a rise in C3a and C5a transgene production in the transgenic mice. At nine weeks, GFAP levels started to decrease in WT and transgenic mice (Fig. 3A). The increased expression of GFAP at five weeks in the transgenic mice may suggest that C3a and C5a are inducing proliferation, activation or migration of astrocytes; however five weeks was the only timepoint where C3a and C5a transgenic mice showed a significant difference in kinetics from WT mice (Fig. 3A and 3B). These results would suggest that C3a and C5a are not playing a significant role in activation and/or proliferation of astrocytes during the course of cuprizone treatment.

We found that microglial staining was greatly increased in C3a and C5a transgenic mice beginning at five weeks (Fig. 3C and 3D) and continuing through seven weeks (Fig. 3C). At five weeks, there was a 2.2-fold and 2.6-fold increase in C5a and C3a transgenic RCA staining, respectively (Fig. 3C). Surprisingly, microglial infiltration in the C3a transgenic mice surpassed levels found in C5a transgenic mice at five weeks (Fig. 3C and 3D). RCA staining in the WT mice was greatest at four weeks and decreased throughout the rest of the study (Fig. 3C). These findings were similar to what our lab has shown in previous cuprizone studies (Briggs et al., 2007). Conversely, the peak of microglial infiltration occurred at five weeks in both C3a and C5a transgenic groups (Fig. 3C). Again, we saw no differences between untreated mice from WT and transgenic groups, suggesting there were not increased levels of GFAP or microglia in the corpus callosum of the transgenics prior to cuprizone treatment (Fig. 3A–D). The highly elevated levels of RCA staining in the corpus callosum of C3a and C5a transgenic mice during demyelination, suggests both C3a and C5a stimulate migration and/or proliferation of microglia during cuprizone treatment.

### 3.3. C3a and C5a expression in the corpus callosum leads to increased oligodendrocyte numbers during early remyelination

It has previously been shown that cuprizone treatment leads to oligodendrocyte apoptosis in the corpus callosum beginning two weeks after initiation of cuprizone treatment (Mason et al., 2000). Oligodendrocyte progenitors begin to increase in the corpus callosum at four weeks, which is why some remyelination occurs before removal of cuprizone from the diet. However, mature oligodendrocytes do not return to levels found in untreated mice until eight to ten weeks of a typical cuprizone study (Mason et al., 2000). When we used an antibody against the transcription factor Olig-2, which is present in both oligodendrocyte progenitors and mature oligodendrocytes, we found that the decrease in oligodendrocyte numbers during cuprizone treatment was similar in WT and both groups of transgenic mice (Fig. 4A). These results would suggest that oligodendrocyte death is a function of the cuprizone toxicity and was not affected by increased C3a or C5a levels. During early remyelination events at week six of cuprizone treatment, we found that C3a and C5a transgenic mice had increased numbers of oligodendrocytes in the corpus callosum compared to WT mice (Fig. 4A and 4B). Oligodendrocyte numbers remained elevated in C3a and C5a transgenic mice through week eight of the study (Fig. 4A). Increased oligodendrocyte numbers may be required in the C3a and C5a transgenic mice for complete remyelination, due to the increased severity of demyelination in the corpus callosum. Interestingly, when we calculated the percentage of total cells that are Olig-2$^+$ cells, we found that there was a significantly higher percentage of Olig-2$^+$ cells in the WT mice at five weeks (Fig. 4C). These findings are most likely due to the increased number of microglia in the corpus callosum of C3a and C5a transgenic mice at five weeks, thus making the ratio of oligodendrocytes to total cells decrease in the transgenic mice. The percentages of cells that are positive for Olig-2 began to increase at five weeks and were not significantly different between WT and transgenic mice between six and ten weeks (Fig. 4C).

### 3.4. C3a and C5a induce cytokine and chemokine production in mixed glia and BV-2 microglia

Our *in vivo* data suggest that C3a and C5a are playing a role in glial cell activation and migration. Previous findings have shown that C5a can induce downstream functions in glial cells, such as chemotaxis and upregulation of cytokine expression (Armstrong et al., 1990; Jauneau et al., 2003; Yao et al., 1990). To determine the role of C3a and/or C5a stimulation on individual glial cell subsets, we treated cells with recombinant C3a and/or C5a. We also treated mixed glia, which contain astrocytes, microglia and oligodendrocyte progenitors, to gain insight on how cellular interaction may play a role in regulating the cytokine response to C3a and/or C5a stimulation. We found that glial cells were capable of upregulating proinflammatory chemokines and cytokines. Mixed glial cultures produced the proinflammatory cytokine IL-6 in response to C3a or C5a 24 hours after treatment (Suppl. Fig. 1 and Suppl. Table 1). These data were verified using an IL-6 ELISA (Fig. 5A). We observed a significant additive effect when cells were treated with C3a and C5a in combination. We also found that mixed glial cultures produced CCL4 (MIP-1β) in response to C5a treatment (Fig. 5A). Interestingly, when cells were treated with C3a there was less CCL4 present in the supernatant after 24 hours compared to untreated cells (Fig. 5A). 72 hours after treatment, BV-2 microglial cultures treated with C5a, C3a or a combination of C3a and C5a had increased expression of CCL4 in cell supernatants compared to untreated control (Suppl. Fig. 1 and Fig. 5B). We did not detect any significant additive effects on CCL4 production when BV-2 cells were treated with both C3a and C5a (Fig. 5B).

When primary astrocytes were treated with C3a and/or C5a, we found that none of the cytokines tested for were increased upon treatment with C3a and/or C5a; however, we found

that the presence of C3a and/or C5a decreased cytokine levels in astrocyte cultures. After one day of treatment, IL-13 was decreased in astrocyte cultures treated with C3a, C5a, or both proteins (Suppl. Fig. 1 and Suppl. Table 3). At day six we found decreases in IL-13, IL-9 and CCL4 (Suppl. Fig. 1 and Suppl. Table 3). We verified the CCL4 multiplex data using an ELISA and similar to our multiplex results, after six days we found CCL4 levels were decreased in cultures treated with C3a and/or C5a (Fig. 5C).

### 3.5. C3a and C5a activate MAPK signaling pathways in primary astrocytes and BV-2 microglia

We demonstrated a direct role for C3a and C5a in stimulating cytokine and chemokine production in mixed glia and microglia, therefore we were interested in how C3a and C5a activate signaling pathways in individual subsets of glia. It has been shown that human recombinant C3a and C5a activate MAPK proteins, ERK1/2, in a human astrocyte cell line and human recombinant C5a stimulation can activate ERK2 in primary murine astrocytes (Osaka et al., 1999a; Sayah et al., 2003). When BV-2 cells were stimulated with 50 nM C5a, we found that ERK2 was phosphorylated as early as one minute after treatment (Fig. 6A and 6B). Both ERK1/2 were significantly activated after five minutes of stimulation with C5a. Activation of ERK1/2 was short lived and by 15 minutes the phosphorylation levels of ERK1/2 were equal to levels found in untreated cells (Fig. 6A and 6B). When these cells were treated with 50 nM C3a, we did not see an increase in phosphorylated ERK1/2 at any of the time points tested (data not shown), suggesting 50 nM C3a does not activate the ERK-MAPK pathway in BV-2 microglia. We treated cells for five minutes with C3a concentrations ranging from 0–100nM and still found no increase in phosphorylation of ERK1/2. We also found that p38 and JNK MAPK pathways were not activated in BV-2 cells when stimulated with 50 nM C3a or C5a (data not shown).

When primary astrocytes were treated with 50nM C3a or 50nM C5a, we found that ERK proteins were activated. In contrast to BV-2 cells treated with C3a, significant phosphorylation of ERK2 occurred at 15 minutes (Fig. 6C and 6F). By 60 minutes, pERK1/2 levels were decreased to levels seen in untreated control cells. When astrocytes were treated with 50nM C5a, levels of pERK1 were higher than untreated control cells starting at 15 minutes (Fig. 6D and 6F). Levels of pERK1/2 were not significantly higher than untreated control cells at 30 minutes ($p = 0.08$ for both pERK1/2), but both ERK1/2 were significantly activated at 60 minutes. We found that the basal levels of ERK1/2 phosphorylation were higher in untreated primary astrocytes compared to BV-2 cells, thus making the overall fold-increase less in primary astrocytes. We also looked for activation of p38 and JNK proteins. We found that p38 MAPK was not phosphorylated in C3a or C5a treated cells (data not shown). Interestingly, we found that JNK1 was phosphorylated in primary astrocytes treated with C3a or C5a (Fig. 6C, 6D and 6E). Similar to ERK1/2 activation, significant activation of JNK1 occurred between 15 and 30 minutes. At 60 minutes after C3a or C5a treatment, JNK1 phosphorylation was not significantly higher than untreated cells. JNK2/3 were not activated in C3a or C5a stimulated primary astrocytes.

## 4. Discussion

It has been previously established that C3a and C5a receptors are upregulated in patients with MS (Gasque et al., 1998; Muller-Ladner et al., 1996) and complement deposition is present within MS lesions (Ingram et al., 2008; Lucchinetti et al., 2000). These results would suggest that C3a and/or C5a could potentially play a role in demyelination, lesion pathology and subsequent remyelination. In the present study we have shown that the C3a and C5a exacerbate demyelination severity in the murine cuprizone model. The expression of C3a or C5a during demyelination amplified microglial staining in the corpus callosum. C3a transgenic mice tended to have greater demyelination severity and higher microglial levels

in the corpus callosum compared to C5a transgenic mice, although these results were not statistically significant (Fig. 1 and Fig. 3). Previous *in vivo* data have suggested a role for C3a and C3aR in diseases affecting the CNS, however it is not clear how C3a mediates its effects within the CNS. There have been no published reports indicating C3a involvement in glial cell migration and results from our lab suggest that recombinant murine C3a does not induce significant migration of BV-2 microglia, primary astrocytes or mixed glia (unpublished results), suggesting chemotaxis may not be the primary effector function of C3a. Previous studies have shown that when astrocytes (Jauneau et al., 2006) and microglia (Heese et al., 1998) are stimulated with C3a, production of growth factors are upregulated, suggesting C3a has the potential to induce cytokine and chemokine production in glia. In the present report, we found that when BV-2 microglia were treated with C3a, CCL4, CCL5 and CCL11 were increased in cell supernatants (Suppl. Fig. 1 and Fig. 5). Microglia have previously been shown to express CCR3 and CCR5, receptors for CCL4 and CCL5 (Albright et al., 1999). Astrocytes also express CCR3, in addition to CCR1, another receptor for CCL5 (Flynn et al., 2003; Han et al., 2000). Additionally, previous cuprizone studies have shown that chemokine mRNA transcripts are upregulated in the brain during cuprizone treatment; including, CCL4 and CCL5 (Biancotti et al., 2008; McMahon et al., 2001). The expression of chemokine receptors on glia in conjunction with upregulated chemokine production by C3a stimulated microglia *in vitro* may be a potential mechanism by which C3a indirectly induces migration of reactive microglia and astrocytes to the demyelinating corpus callosum during cuprizone treatment. Overall, our *in vivo* data suggest C3a induces a proinflammatory response, exacerbating demyelination. In contrast, previous data have shown that C3a-GFAP mice are protected from LPS-induced shock (Boos et al., 2005), suggesting that C3a expressed in the CNS is capable of inducing a protective response, as well. Therefore, depending on the stimuli in the CNS, C3a can induce harmful or protective outcomes.

It has been established that C5a mediates migration of microglia and astrocytes *in vitro* (Armstrong et al., 1990; Nolte et al., 1996; Yao et al., 1990), which could explain the increased levels of RCA staining and GFAP expression we observed in the corpus callosum of C5a transgenic mice during demyelination (Fig. 3). Alternatively, cytokine and chemokine production were upregulated in mixed glial and BV-2 cell cultures stimulated with C3a or C5a (Suppl. Fig. 1 and Fig. 5). Similar to results found when cells were treated with C3a, chemokines that were upregulated in these cell cultures included CCL4, CCL5 and CCL11. The ability of glia to produce chemokines in response to C5a presents another possible mechanism for the observed increase in cellularity in the corpus callosum during demyelination. Future studies will be required to determine if these chemokines are necessary for demyelination events in the cuprizone model. Previous results showed that C5a and C5aR do not exacerbate disease severity in the EAE model (Reiman et al., 2005; Reiman et al., 2002). The disparity between our results and those found in the EAE model most likely reflect the differences in the induction of demyelination and differing effector mechanisms between the two models. There are different lesion types found in MS (Lucchinetti et al., 2000) and both models address different aspects of lesion pathology.

In a recent report, it was found that CXCR2^{+} neutrophils are necessary for demyelination in the cuprizone model (Liu et al., 2010). This is the first report of neutrophils being present within the brain during cuprizone treatment. Neutrophil numbers peaked in the corpus callosum early at five days after initiation of cuprizone treatment. It has been well established that C5a is a potent chemoattractant for neutrophils (Gerard and Gerard, 1994; Guo and Ward, 2005), so it is possible that in addition to increased microglia, neutrophil numbers may also be increased and mediating some effect on the exacerbated demyelination observed in C5a transgenic mice during cuprizone treatment. It has not yet been established

how CXCR2^{+} neutrophils mediate their effect within the corpus callosum during demyelination in the cuprizone model.

In contrast to the proinflammatory cytokine and chemokine production we found in C3a and/or C5a-stimulated microglia and mixed glia, astrocytes treated with C3a and/or C5a exhibited regulatory characteristics. Untreated astrocyte supernatants had greater levels of IL-9, IL-13 and CCL4 compared to astrocytes that were treated with C3a or C5a (Suppl. Fig. 1 and Fig. 5), suggesting C3a and C5a stimulation may result in down modulation of cytokine production in these cells. Other studies have shown that when astrocytes are stimulated with proinflammatory mediators, astrocytes can act in a regulatory manner through production of regulatory cytokines (Bsibsi et al., 2006) or induction of regulatory signaling pathways (Qin et al., 2008; Stark et al., 2004). Additionally, it has been shown that when pituitary cell cultures are treated with C3a, the production of hormones involved in the control of inflammation are increased (Francis et al., 2003). We found when primary astrocytes were treated with C3a and/or C5a they did not upregulate any cytokines that are considered to be anti-inflammatory, including the regulatory cytokine IL-10 (Suppl. Fig. 3). Even though primary astrocytes are downregulating cytokine production, the ability of mixed glial cultures to produce proinflammatory cytokines and chemokines in response to C3a and/or C5a treatment *in vitro* would suggest that the proinflammatory response, which is most likely due to microglial activation, overrides the regulatory response of astrocytes, the most prevalent cell type in mixed glial cultures. Alternatively, astrocytes may require cellular interaction with other types of glia to upregulate cytokine and chemokine production in response to C3a and C5a stimulation. We found that MAPK pathways are differentially activated in astrocytes and BV-2 microglia (Fig. 6), yet further investigation into C3a and C5a-mediated activation of alternative signaling pathways are needed to determine which signal transduction pathways are required for suppressing cytokine production by astrocytes.

We established that both C3a and C5a exacerbate demyelination pathogenesis; however their role in remyelination is complex. Although transgenic mice had worse demyelination severity through seven weeks, we found that C3a and C5a transgenic mice were able to remyelinate as effectively as WT mice. Interestingly, we found that oligodendrocytes returned to the corpus callosum of transgenic mice in greater numbers than WT mice at six through eight weeks of the study. Previous studies have shown that C5a does not induce chemotaxis of oligodendrocytes progenitors *in vitro* (Armstrong et al., 1990) and we did not see significant increases of oligodendrocytes in the corpus callosum until six weeks of the cuprizone study, suggesting chemotaxis to C3a or C5a is not the primary mechanism for the increase in oligodendrocytes in the corpus callosum. There have been studies suggesting some inflammation is necessary for microglia-mediated clearance of apoptotic cells and myelin debris and subsequent remyelination to occur (Neumann et al., 2009). While microglia are thought to be the primary effector cell during demyelination in the cuprizone model, it has also been found that cytokines and growth factors most likely produced by microglia are necessary for remyelination. For instance, IL-1β, LIF and TNF-α, all thought to be produced by microglia and astrocytes, have been shown to enhance remyelination (Arnett et al., 2001; Marriott et al., 2008; Mason et al., 2001). Additionally, growth factors such as, insulin growth factor (IGF) are necessary for remyelination by oligodendrocytes in the cuprizone model (Mason et al., 2003). Therefore, the increase in oligodendrocytes in C3a and C5a transgenic mice could be explained by the increase in proinflammatory microglia in the corpus callosum at five to seven weeks. In the present report, we did not find upregulation of IL-1β or TNF-α when glial cells were stimulated with recombinant C3a and/or C5a *in vitro* (Suppl. Tables). Whether or not C3a or C5a play a role in upregulation of growth factor and cytokine production by glial cells that are necessary for oligodendrocyte migration, maturation or proliferation after demyelination has occurred has yet to be established. Inhibiting C3a and C5a in the CNS of patients with demyelinating

lesions could potentially be of therapeutic value; however the importance of C3a and C5a production during remyelination remains uncertain. Our results would suggest that C3a and C5a enhance recruitment of oligodendrocytes into demyelinated areas, thus these proteins could potentially be harnessed for their beneficial properties in remyelination pathology. These studies are exclusively focused on C3a and C5a proteins and more studies will be necessary to fully evaluate the complex role of the cascade and the various other complement proteins in neuroinflammation.

## Supplementary Material

Refer to Web version on PubMed Central for supplementary material.

## Acknowledgments

## References

Albright AV, Shieh JT, Itoh T, Lee B, Pleasure D, O'Connor MJ, Doms RW, Gonzalez-Scarano F. Microglia express CCR5, CXCR4, and CCR3, but of these, CCR5 is the principal coreceptor for human immunodeficiency virus type 1 dementia isolates. J Virol 1999;73:205–13. [PubMed: 9847323]

Anderson RD, Haskell RE, Xia H, Roessler BJ, Davidson BL. A simple method for the rapid generation of recombinant adenovirus vectors. Gene Ther 2000;7:1034–8. [PubMed: 10871752]

Armstrong RC, Harvath L, Dubois-Dalcq ME. Type 1 astrocytes and oligodendrocyte-type 2 astrocyte glial progenitors migrate toward distinct molecules. J Neurosci Res 1990;27:400–7. [PubMed: 2097382]

Arnett HA, Mason J, Marino M, Suzuki K, Matsushima GK, Ting JP. TNF alpha promotes proliferation of oligodendrocyte progenitors and remyelination. Nat Neurosci 2001;4:1116–22. [PubMed: 11600888]

Bakker DA, Ludwin SK. Blood-brain barrier permeability during Cuprizone-induced demyelination. Implications for the pathogenesis of immune-mediated demyelinating diseases. J Neurol Sci 1987;78:125–37. [PubMed: 3553434]

Biancotti JC, Kumar S, de Vellis J. Activation of inflammatory response by a combination of growth factors in cuprizone-induced demyelinated brain leads to myelin repair. Neurochem Res 2008;33:2615–28. [PubMed: 18661234]

Boos L, Campbell IL, Ames R, Wetsel RA, Barnum SR. Deletion of the complement anaphylatoxin C3a receptor attenuates, whereas ectopic expression of C3a in the brain exacerbates, experimental autoimmune encephalomyelitis. J Immunol 2004;173:4708–14. [PubMed: 15383607]

Boos L, Szalai AJ, Barnum SR. C3a expressed in the central nervous system protects against LPS-induced shock. Neurosci Lett 2005;387:68–71. [PubMed: 16085360]

Briggs DT, Martin CB, Ingersoll SA, Barnum SR, Martin BK. Astrocyte-specific expression of a soluble form of the murine complement control protein Crry confers demyelination protection in the cuprizone model. Glia 2007;55:1405–15. [PubMed: 17674370]

Bsibsi M, Persoon-Deen C, Verwer RW, Meeuwsen S, Ravid R, Van Noort JM. Toll-like receptor 3 on adult human astrocytes triggers production of neuroprotective mediators. Glia 2006;53:688–95. [PubMed: 16482523]

Cianflone K, Xia Z, Chen LY. Critical review of acylation-stimulating protein physiology in humans and rodents. Biochim Biophys Acta 2003;1609:127–43. [PubMed: 12543373]

Davoust N, Jones J, Stahel PF, Ames RS, Barnum SR. Receptor for the C3a anaphylatoxin is expressed by neurons and glial cells. Glia 1999;26:201–11. [PubMed: 10340761]

Flynn G, Maru S, Loughlin J, Romero IA, Male D. Regulation of chemokine receptor expression in human microglia and astrocytes. J Neuroimmunol 2003;136:84–93. [PubMed: 12620646]

Fonseca MI, Ager RR, Chu SH, Yazan O, Sanderson SD, LaFerla FM, Taylor SM, Woodruff TM, Tenner AJ. Treatment with a C5aR antagonist decreases pathology and enhances behavioral performance in murine models of Alzheimer's disease. J Immunol 2009;183:1375–83. [PubMed: 19561098]

Francis K, Lewis BM, Akatsu H, Monk PN, Cain SA, Scanlon MF, Morgan BP, Ham J, Gasque P. Complement C3a receptors in the pituitary gland: a novel pathway by which an innate immune molecule releases hormones involved in the control of inflammation. Faseb J 2003;17:2266–8. [PubMed: 14563692]

Gasque P, Singhrao SK, Neal JW, Gotze O, Morgan BP. Expression of the receptor for complement C5a (CD88) is up-regulated on reactive astrocytes, microglia, and endothelial cells in the inflamed human central nervous system. Am J Pathol 1997;150:31–41. [PubMed: 9006319]

Gasque P, Singhrao SK, Neal JW, Wang P, Sayah S, Fontaine M, Morgan BP. The receptor for complement anaphylatoxin C3a is expressed by myeloid cells and nonmyeloid cells in inflamed human central nervous system: analysis in multiple sclerosis and bacterial meningitis. J Immunol 1998;160:3543–54. [PubMed: 9531317]

Gavrilyuk V, Kalinin S, Hilbush BS, Middlecamp A, McGuire S, Pelligrino D, Weinberg G, Feinstein DL. Identification of complement 5a-like receptor (C5L2) from astrocytes: characterization of anti-inflammatory properties. J Neurochem 2005;92:1140–9. [PubMed: 15715664]

Gerard C, Gerard NP. C5A anaphylatoxin and its seven transmembrane-segment receptor. Annu Rev Immunol 1994;12:775–808. [PubMed: 8011297]

Groebe A, Clarner T, Baumgartner W, Dang J, Beyer C, Kipp M. Cuprizone treatment induces distinct demyelination, astrocytosis, and microglia cell invasion or proliferation in the mouse cerebellum. Cerebellum 2009;8:163–74. [PubMed: 19259754]

Guo RF, Ward PA. Role of C5a in inflammatory responses. Annu Rev Immunol 2005;23:821–52. [PubMed: 15771587]

Haas PJ, van Strijp J. Anaphylatoxins: Their role in bacterial infection and inflammation. Immunol Res 2007;37:161–75. [PubMed: 17873401]

Han Y, Wang J, Zhou Z, Ransohoff RM. TGFbeta1 selectively up-regulates CCR1 expression in primary murine astrocytes. Glia 2000;30:1–10. [PubMed: 10696139]

Heese K, Hock C, Otten U. Inflammatory signals induce neurotrophin expression in human microglial cells. J Neurochem 1998;70:699–707. [PubMed: 9453564]

Hiremath MM, Saito Y, Knapp GW, Ting JP, Suzuki K, Matsushima GK. Microglial/macrophage accumulation during cuprizone-induced demyelination in C57BL/6 mice. J Neuroimmunol 1998;92:38–49. [PubMed: 9916878]

Ingram G, Hakobyan S, Robertson NP, Morgan BP. Complement in multiple sclerosis: its role in disease and potential as a biomarker. Clin Exp Immunol. 2008

Jacob A, Bao L, Brorson J, Quigg RJ, Alexander JJ. C3aR inhibition reduces neurodegeneration in experimental lupus. Lupus 2010a;19:73–82. [PubMed: 19900981]

Jacob A, Hack B, Bai T, Brorson JR, Quigg RJ, Alexander JJ. Inhibition of C5a receptor alleviates experimental CNS lupus. J Neuroimmunol 2010b;221:46–52. [PubMed: 20207017]

Jauneau AC, Ischenko A, Chan P, Fontaine M. Complement component anaphylatoxins upregulate chemokine expression by human astrocytes. FEBS Lett 2003;537:17–22. [PubMed: 12606024]

Jauneau AC, Ischenko A, Chatagner A, Benard M, Chan P, Schouft MT, Patte C, Vaudry H, Fontaine M. Interleukin-1beta and anaphylatoxins exert a synergistic effect on NGF expression by astrocytes. J Neuroinflammation 2006;3:8. [PubMed: 16594997]

Klos A, Tenner AJ, Johswich KO, Ager RR, Reis ES, Kohl J. The role of the anaphylatoxins in health and disease. Mol Immunol 2009;46:2753–66. [PubMed: 19477527]

Kondo A, Nakano T, Suzuki K. Blood-brain barrier permeability to horseradish peroxidase in twitcher and cuprizone-intoxicated mice. Brain Res 1987;425:186–90. [PubMed: 3427420]

Ligon KL, Alberta JA, Kho AT, Weiss J, Kwaan MR, Nutt CL, Louis DN, Stiles CD, Rowitch DH. The oligodendroglial lineage marker OLIG2 is universally expressed in diffuse gliomas. J Neuropathol Exp Neurol 2004;63:499–509. [PubMed: 15198128]

Liu L, Belkadi A, Darnall L, Hu T, Drescher C, Cotleur AC, Padovani-Claudio D, He T, Choi K, Lane TE, Miller RH, Ransohoff RM. CXCR2-positive neutrophils are essential for cuprizone-induced demyelination: relevance to multiple sclerosis. Nat Neurosci 2010;13:319–26. [PubMed: 20154684]

Lucchinetti C, Bruck W, Parisi J, Scheithauer B, Rodriguez M, Lassmann H. Heterogeneity of multiple sclerosis lesions: implications for the pathogenesis of demyelination. Ann Neurol 2000;47:707–17. [PubMed: 10852536]

Marriott MP, Emery B, Cate HS, Binder MD, Kemper D, Wu Q, Kolbe S, Gordon IR, Wang H, Egan G, Murray S, Butzkueven H, Kilpatrick TJ. Leukemia inhibitory factor signaling modulates both central nervous system demyelination and myelin repair. Glia 2008;56:686–698. [PubMed: 18293407]

Mason JL, Jones JJ, Taniike M, Morell P, Suzuki K, Matsushima GK. Mature oligodendrocyte apoptosis precedes IGF-1 production and oligodendrocyte progenitor accumulation and differentiation during demyelination/remyelination. J Neurosci Res 2000;61:251–62. [PubMed: 10900072]

Mason JL, Suzuki K, Chaplin DD, Matsushima GK. Interleukin-1beta promotes repair of the CNS. J Neurosci 2001;21:7046–52. [PubMed: 11549714]

Mason JL, Xuan S, Dragatsis I, Efstratiadis A, Goldman JE. Insulin-like growth factor (IGF) signaling through type 1 IGF receptor plays an important role in remyelination. J Neurosci 2003;23:7710–8. [PubMed: 12930811]

Matsushima GK, Morell P. The neurotoxicant, cuprizone, as a model to study demyelination and remyelination in the central nervous system. Brain Pathol 2001;11:107–16. [PubMed: 11145196]

McCarthy KD, de Vellis J. Preparation of separate astroglial and oligodendroglial cell cultures from rat cerebral tissue. J Cell Biol 1980;85:890–902. [PubMed: 6248568]

McMahon EJ, Cook DN, Suzuki K, Matsushima GK. Absence of macrophage-inflammatory protein-1alpha delays central nervous system demyelination in the presence of an intact blood-brain barrier. J Immunol 2001;167:2964–71. [PubMed: 11509646]

Morell P, Barrett CV, Mason JL, Toews AD, Hostettler JD, Knapp GW, Matsushima GK. Gene expression in brain during cuprizone-induced demyelination and remyelination. Mol Cell Neurosci 1998;12:220–7. [PubMed: 9828087]

Mukherjee P, Thomas S, Pasinetti GM. Complement anaphylatoxin C5a neuroprotects through regulation of glutamate receptor subunit 2 in vitro and in vivo. J Neuroinflammation 2008;5:5. [PubMed: 18230183]

Muller-Ladner U, Jones JL, Wetsel RA, Gay S, Raine CS, Barnum SR. Enhanced expression of chemotactic receptors in multiple sclerosis lesions. J Neurol Sci 1996;144:135–41. [PubMed: 8994115]

Nataf S, Levison SW, Barnum SR. Expression of the anaphylatoxin C5a receptor in the oligodendrocyte lineage. Brain Res 2001;894:321–6. [PubMed: 11251209]

Neumann H, Kotter MR, Franklin RJ. Debris clearance by microglia: an essential link between degeneration and regeneration. Brain 2009;132:288–95. [PubMed: 18567623]

Nikcevich KM, Piskurich JF, Hellendall RP, Wang Y, Ting JP. Differential selectivity of CIITA promoter activation by IFN-gamma and IRF-1 in astrocytes and macrophages: CIITA promoter activation is not affected by TNF-alpha. J Neuroimmunol 1999;99:195–204. [PubMed: 10505975]

Nolte C, Moller T, Walter T, Kettenmann H. Complement 5a controls motility of murine microglial cells in vitro via activation of an inhibitory G-protein and the rearrangement of the actin cytoskeleton. Neuroscience 1996;73:1091–107. [PubMed: 8809827]

Osaka H, McGinty A, Hoepken UE, Lu B, Gerard C, Pasinetti GM. Expression of C5a receptor in mouse brain: role in signal transduction and neurodegeneration. Neuroscience 1999a;88:1073–82. [PubMed: 10336122]

Osaka H, Mukherjee P, Aisen PS, Pasinetti GM. Complement-derived anaphylatoxin C5a protects against glutamate-mediated neurotoxicity. J Cell Biochem 1999b;73:303–11. [PubMed: 10321830]

Qin H, Niyongere SA, Lee SJ, Baker BJ, Benveniste EN. Expression and functional significance of SOCS-1 and SOCS-3 in astrocytes. J Immunol 2008;181:3167–76. [PubMed: 18713987]

Rahpeymai Y, Hietala MA, Wilhelmsson U, Fotheringham A, Davies I, Nilsson AK, Zwirner J, Wetsel RA, Gerard C, Pekny M, Pekna M. Complement: a novel factor in basal and ischemia-induced neurogenesis. Embo J 2006;25:1364–74. [PubMed: 16498410]

Reiman R, Campos Torres A, Martin BK, Ting JP, Campbell IL, Barnum SR. Expression of C5a in the brain does not exacerbate experimental autoimmune encephalomyelitis. Neurosci Lett 2005;390:134–8. [PubMed: 16154690]

Reiman R, Gerard C, Campbell IL, Barnum SR. Disruption of the C5a receptor gene fails to protect against experimental allergic encephalomyelitis. Eur J Immunol 2002;32:1157–63. [PubMed: 11932923]

Sayah S, Jauneau AC, Patte C, Tonon MC, Vaudry H, Fontaine M. Two different transduction pathways are activated by C3a and C5a anaphylatoxins on astrocytes. Brain Res Mol Brain Res 2003;112:53–60. [PubMed: 12670702]

Shinjyo N, Stahlberg A, Dragunow M, Pekny M, Pekna M. Complement-derived anaphylatoxin C3a regulates in vitro differentiation and migration of neural progenitor cells. Stem Cells 2009;27:2824–32. [PubMed: 19785034]

Sidman, RL.; Abervine, JB.; Pierce, ET. Atlas of the Mouse Brain and Spinal Cord. Harvard University Press; Cambridge, MA: 1971.

Sospedra M, Martin R. Immunology of multiple sclerosis. Annu Rev Immunol 2005;23:683–747. [PubMed: 15771584]

Stark JL, Lyons JA, Cross AH. Interferon-gamma produced by encephalitogenic cells induces suppressors of cytokine signaling in primary murine astrocytes. J Neuroimmunol 2004;151:195–200. [PubMed: 15145618]

Torkildsen O, Brunborg LA, Myhr KM, Bo L. The cuprizone model for demyelination. Acta Neurol Scand Suppl 2008;188:72–6. [PubMed: 18439226]

Trapp BD, Nave KA. Multiple sclerosis: an immune or neurodegenerative disorder? Annu Rev Neurosci 2008;31:247–69. [PubMed: 18558855]

Woodruff TM, Costantini KJ, Crane JW, Atkin JD, Monk PN, Taylor SM, Noakes PG. The complement factor c5a contributes to pathology in a rat model of amyotrophic lateral sclerosis. J Immunol 2008;181:8727–34. [PubMed: 19050293]

Yao J, Harvath L, Gilbert DL, Colton CA. Chemotaxis by a CNS macrophage, the microglia. J Neurosci Res 1990;27:36–42. [PubMed: 2254955]
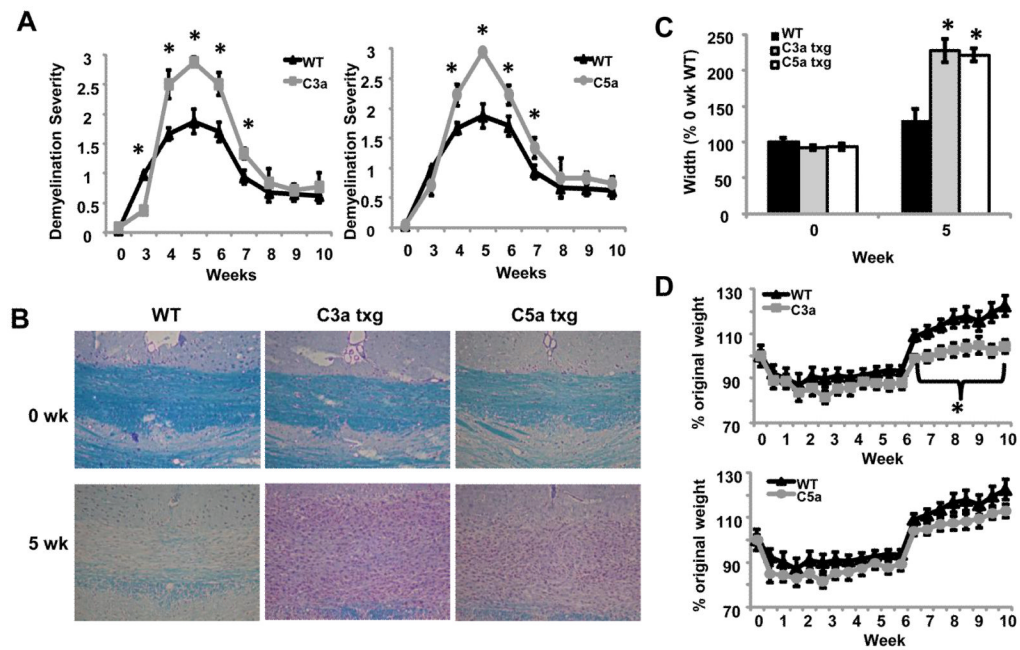
**Figure 1.**
Increased levels of C3a and C5a in the brain lead to exacerbated demyelination and delayed remyelination in the cuprizone model. (A) Mice were treated with cuprizone for the indicated times and the brains were harvested. 5µm sections were stained using LFB-PAS and evaluated by microscopy. The stained sections were blindly scored by three individuals and averaged. Four to eight mice were analyzed per time point for each experimental group. (B) Representative images of LFB-PAS staining at zero and five weeks of cuprizone treatment. Four to eight mice were analyzed for each experimental group. (C) The extent of inflammation in and surrounding the corpus callosum at zero and five weeks was measured in µm using NIS Elements 3.1 Imaging software. In this figure, 100% is the mean width of the inflammatory lesion at midline of the untreated WT group. Four to eight mice were analyzed for each experimental group. (D) Weight of WT and transgenic mice throughout cuprizone treatment. Mice were weighed bi-weekly throughout the ten week study, n = 7–16 mice per group. Statistical significance was calculated using unpaired Student's t-test and one-way ANOVA, * $p < 0.05$. Error bars represent standard deviation.
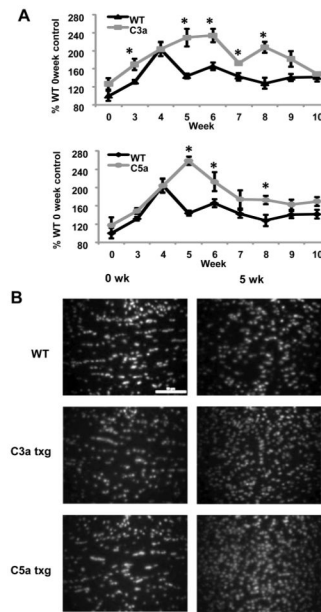
**Figure 2.**
C3a and C5a expression leads to increased cellular infiltration into the corpus callosum during cuprizone treatment. (A) 5μm sections were stained with DAPI nuclear stain and the cell number was quantified NIS Elements 3.1 Imaging software. The results are presented as percent increase over untreated WT control. (B) Representative images of DAPI staining at zero and five weeks of cuprizone treatment. The scale bar equals 50μm. Statistical significance was calculated using unpaired Student's t-test and one-way ANOVA, * $p < 0.05$, n= four to eight mice were used per time point for each experimental group in the above experiments and the error bars represent standard deviation.
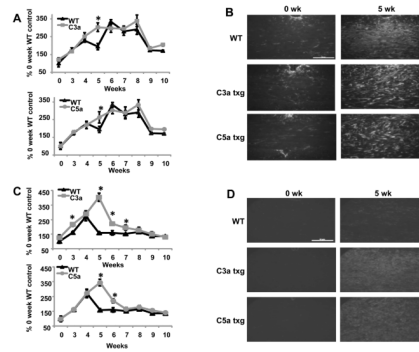
**Figure 3.**
Transgenic expression of C3a or C5a in the corpus callosum leads to increased microglia and GFAP expression. (A) Sections were stained with antibody against GFAP and the mean fluorescence intensities measured. The results are shown as a percent increase over untreated WT control. (B) Representative images of GFAP staining at zero and five weeks of cuprizone treatment. (C) 5μm sections were stained with RCA lectin and the mean fluorescence intensities measured. The results are shown as the percent increase over untreated WT control. (D) Representative images of RCA staining at zero and five weeks of cuprizone treatment. The scale bars equal 50μm. Statistical significance was calculated using unpaired Student's t-test and one-way ANOVA, * $p < 0.05$, n= four to eight mice were used for each time point for each experimental group in the above experiments and the error bars represent standard deviation.
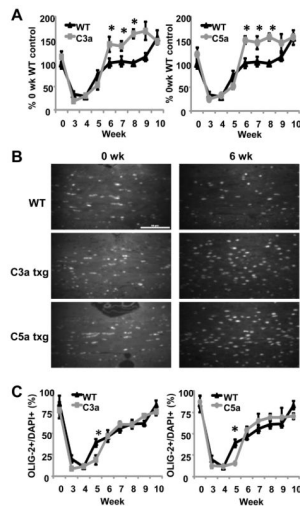
**Figure 4.**
Oligodendrocyte numbers are increased during early remyelination in C3a and C5a transgenic mice. (A) Sections were stained with Olig-2 antibody. The numbers of Olig-2^{+} cells were quantified in a predetermined area of the corpus callosum below the midline of the brain using NIS Elements 3.1 Imaging software. The results are presented as a percent change from WT untreated mice. (B) Representative images of Olig-2 staining at zero and six weeks of cuprizone treatment. (C) Olig-2^{+} cells as a percentage of total DAPI^{+} cells. The same area of the corpus callosum was used for both DAPI and Olig-2 quantification. The scale bar equals 50μm. Statistical significance was calculated using unpaired Student's t-test and one-way ANOVA, * $p < 0.05$. At each time point four to eight mice were analyzed for each experimental group and the error bars represent standard deviation.
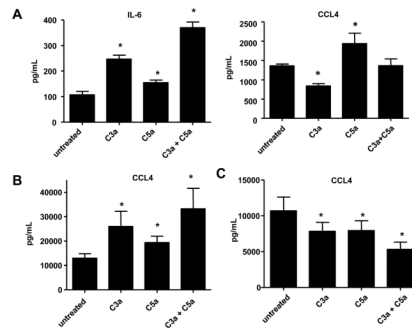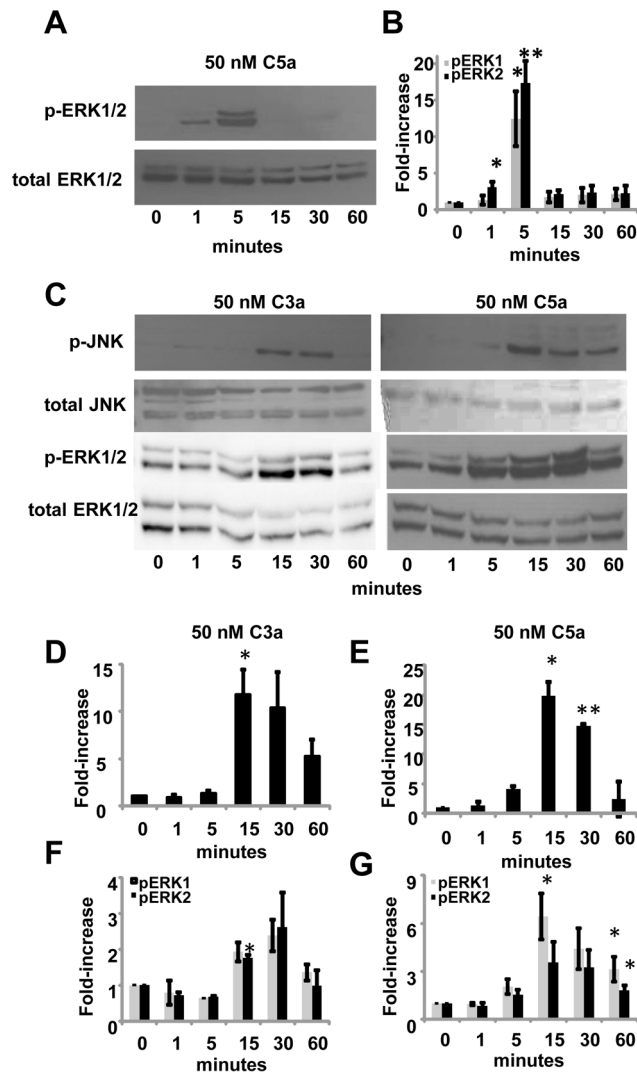
**Figure 5.**
C3a and C5a induce cytokine and chemokine production in mixed glia and BV-2 microglia. (A) Mixed glia were treated with 50nM C3a, 50nM C5a or a combination of 50nM C3a and C5a for 24 hours. After 24 hours of treatment, supernatants were collected and used in ELISAs specific for IL-6 or CCL4 (B) BV-2 microglia were treated with 50nM C3a, 50nM C5a or a combination of 50nM C3a and C5a for 72 hours. After 72 hours of treatment, supernatants were collected and used in an ELISA specific for CCL4. (C) Primary astrocytes were stimulated with 50nM C3a, 50nM C5a or a combination of 50nM C3a and C5a. After 144 hours, cell supernatants were collected from the cell cultures and analyzed using an ELISA specific for CCL4. Samples from three experiments were used for ELISAs. Statistical significance was calculated using unpaired student's t-test, * $p < 0.05$. Error bars represent standard deviation.

**Figure 6.**
C3a and C5a activate MAPK signaling pathways in primary astrocytes and BV-2 microglia. (A) BV-2 cells were stimulated with 50nM C5a for 0–60 minutes and whole cell lysates were used to analyze ERK1/2 activation by immunoblotting. After pERK1/2 were detected, all blots were stripped and re-probed for total ERK1/2. (B) The density of each band was measured using ImageJ software. Phosphorylated values were normalized to total values to account for any discrepancies in protein loading. Three blots from three different experiments were used for measuring ERK1/2 activation. (C) Primary astrocytes were stimulated with 50nM C3a or 50nM C5a for 0–60 minutes. Whole cell lysates were used to analyze phosphorylated ERK1/2 or JNK by immunoblotting. All blots were stripped and reprobed for total ERK1/2 or total JNK. (D) Phosphorylated values for pJNK from primary astrocytes treated with 50nM C3a or (E) 50nM C5a were normalized to total JNK values to account for any differences in protein loading. (F) Phosphorylated values for pERK1/2 from primary astrocytes treated with 50nM C3a or (G) 50nM C5a were normalized to total ERK1/2 values to account for protein loading errors. Statistical significance was calculated using unpaired student's t-test, ** $p < 0.001$, * $p < 0.05$. Three or more blots were used for measuring ERK1/2 or JNK activation in primary astrocytes. Error bars represent standard deviation.